

Introducing Composite Structures Using Newly Developed Checkered Steel Pipe and Deformed Flange H-shapes*

Masakatsu SATO**
Masao ISHIWATA**

Michihiko HARA**
Eisuke YAMANAKA***

For a steel-concrete composite structure, a fail-safe mechanism of stress transmission in the steel-concrete interface is of primary importance. The authors have developed H-shapes with deformed flange surfaces and steel pipes with checkered projections on their surfaces as a means of increasing bond resistance with concrete.

The composite new steel pipes and the encased new H composite beams have been subjected to several kinds of tests including pull-out, push-out and bending, and the following points are confirmed:

- (1) Checkered projection is found to be significantly effective in resisting push-out and bending loads.*
- (2) The mechanical properties of the encased deformed flange H composite beams are found to be at most equivalent to that of reinforced concrete beams using large-diameter deformed bars.*

1 Introduction

Today, steel-concrete composite structures are widely used as materials for civil engineering and building because of a rational combination of the advantageous characteristics of both elements; steel's tensile strength and toughness, concrete's compressive strength and stiffness, and composite structure's noise and vibration absorption and high corrosion resistance properties. Composite girders used in bridges, concrete encased steel skeletons and reinforcing bars (called SRC) beams applied in buildings are well known, but composite piles used in foundations and main pipes of jackets and piers in marine structures are important new applications in Japan.

It is of primary importance that a steel-concrete composite structure be provided with an effective stress transmission mechanism in its steel-concrete interface. The bond strength between steel and con-

crete may be increased through either mechanical shear connectors as used in composite girders¹⁾ or surface deformations as of deformed bar²⁾. The latter has a decisive advantage in work convenience and material saving, and therefore, any substantial improvement in steel-concrete bond must be derived from the optimum selection of steel surface projections. The optimum pattern and height of projections on steel surface must be determined through the selection of an optimum combination of projections shape based on service conditions including the minimum bond strength requirements, and manufacturing conditions including rolling load capacity.

The authors developed rolled H-shapes, as shown in Fig. 1, with lateral projections on the outside surface of both flanges (called deformed flange H-shapes) and steel pipe with checkered projections on its surface (called checkered steel pipe) as a means of increasing bond resistance.

In this paper, concrete bonding effects of deformed flange H-shapes and checkered steel pipe are explained, and structural behavior, including fatigue characteristics, of composite checkered steel pipe and encased deformed flange H composite beams are described.

* Rearranged with following two articles: (1) *Kawasaki Steel Giho*, 12 (1980) 4, pp. 77-92, (2) *ibid.*, 13 (1981) 1, pp. 179-193

** Engineering Division

*** Mizushima Works

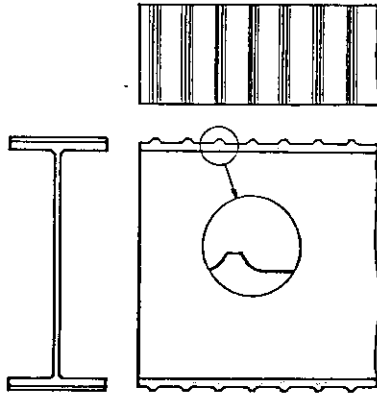


Fig. 1 Schema of deformed flange H-shapes with lateral projection

2 Selection of Projection Shapes

2.1 Pull-out Tests for Flat and Lugged Steel Plates³⁾

The bond characteristics of lugged plates are considerably affected by such factors as the height (h), spacing (d) and setting angle (θ) of projection, and it has been empirically confirmed that the influence of θ

is negligible when it is not less than 50° . In the present pull-out tests where θ was set at 60° with h and d adopted as parameters, 19 sets of steel plates with lateral projections, including deformed flange plates of H-shapes, and checkered plate, all of which are shown in Table 1, were used. Fig. 2 shows the projection pattern and configuration of checkered projection plate.

The maximum coarse aggregate size was 25 mm, and the design strength of the concrete (σ_c) was 30 MPa. Following four weeks of air curing, pull-out tests were performed to determine the relationship between bond stress (τ_b) and slippage at the free end (δ_f).

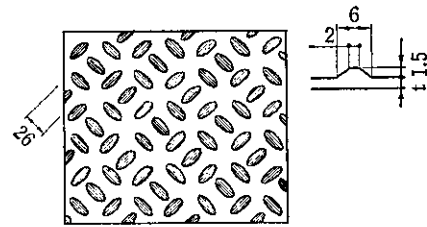


Fig. 2 Schema of checkered projection plate

Table 1 Parameter of specimens, and experimental results on pull-out tests

Specimen	Projection(mm)		Steel pipe		Bond stress(MPa)		Remark
	Height h (mm)	Space d (mm)	Diameter ϕ (mm)	Length l (mm)	$\delta_f=0.05$ mm	$\delta_f=1.00$ mm	
A-0	0	∞	267	300	2.2	2.4	Flat plate
A-1.5-a	1.5	7.5	"	"	10.1	14.5	Lateral projection
b	"	15	"	"	8.6	16.5	"
c	"	22	"	"	6.0	13.8	"
d	"	30	"	"	5.0	10.9	"
A-3.0-a	3.0	15	"	"	11.6	18.1	"
b	"	30	"	"	7.1	17.1	"
c	"	45	"	"	5.1	13.7	"
d	"	60	"	"	4.7	11.1	"
A-4.5-a	4.5	22	"	"	10.3	18.2	"
b	"	45	"	"	7.5	16.3	"
c	"	67	"	"	7.2	16.2	"
d	"	90	"	"	6.8	13.4	"
A-6.0-a	6.0	30	"	"	11.0	20.6	"
b	"	60	"	"	7.5	16.9	"
c	"	90	"	"	7.0	15.6	"
CH1	1.5	28	"	"	6.1	12.7	Checkered plate (Ref. Fig.2)
LH2	3.5	18	"	"	11.5	20.5	Deformed flange H (Ref. Fig.1)
D51	3.5	15	"	"	8.4	15.5	D51 deformed bar
D-4.5-b	"	"	"	200	6.8	17.2	Lateral projection
E-4.5-b	"	"	400	300	9.0	17.2	"
F-4.5-b	"	"	100	"	8.2	16.2	"

2.2 Bond Strength between Concrete and Lugged Steel Plates

The relationship between τ_b and δ_f in pull-out tests is shown in Fig. 3.

Bond resistance of flat steel plates depends on inherent adhesion functioning on the steel-concrete interface, such as agglutination and friction. Much of it is on the latter. Consequently, as the steel plates begin to slip, the amount of slippage rises sharply to reach the maximum bond stress ($\tau_{b,max}$). On the other hand, lugged steel plates are designed to reinforce mechanical resistance to slippage by means of projections. A phenomenon in which the amount of slippage at the free end sharply increases immediately after relative slippage is generated, is not observed. Slippage increases in proportion to the load. Hence, in lugged steel plates, it can be said that rather than $\tau_{b,max}$, τ_b with respect to the specific amount of slippage is crucial.

The relation of τ_b corresponding to numerous δ_f with projection space d is shown in Fig. 4. From this diagram, it can be seen that τ_b is roughly in inverse proportion to d and that τ_b grows as h/d increases. Now, the relation of τ_b with h/d when δ_f is 0.05 mm and 1.00 mm is arranged and shown in Fig. 5. From this diagram, equation (1) is obtained.

$$\left. \begin{aligned} \tau_b \text{ (MPa)} &= 3 + 50 \cdot (h/d) \\ &\quad \text{at } \delta_f = 0.05 \text{ mm} \\ \tau_b \text{ (MPa)} &= 9 + 72 \cdot (h/d) \\ &\quad \text{at } \delta_f = 1.00 \text{ mm} \end{aligned} \right\} \dots (1)$$

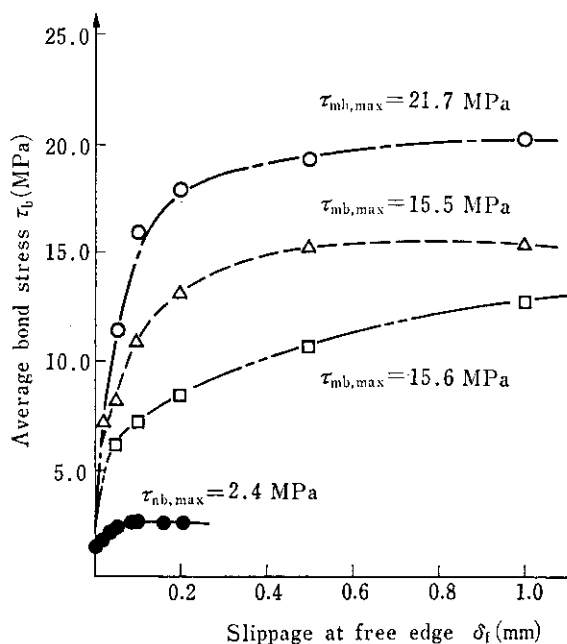


Fig. 3 Relation between bond stress and slippage at free edge in pull-out tests

2.3 Shapes of Projection on H-shapes and Checkered Plates

On the basis of the results of these experiments, as shown in Figs. 4 and 5, and studies regarding lugged steel plates, 3.0 mm and 18 mm have been adopted as lateral projection height and the space on deformed flange surface of H-shapes, respectively.

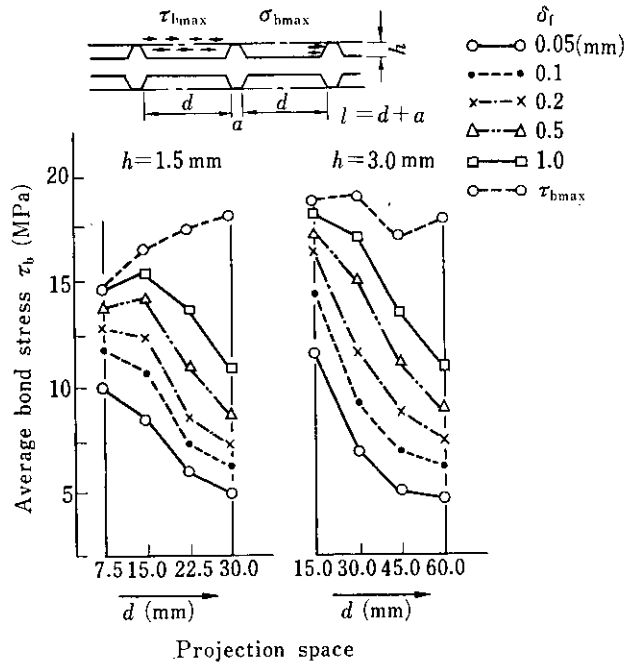
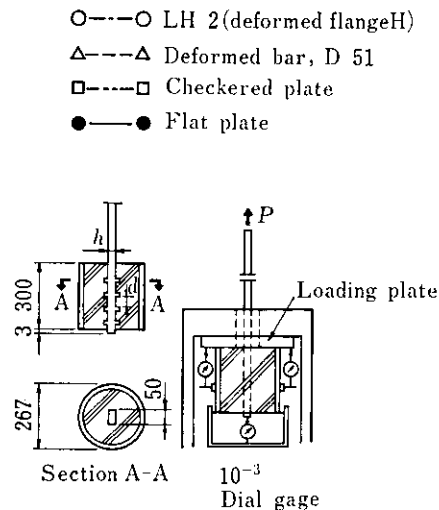


Fig. 4 Relations between average bond stress and projection space



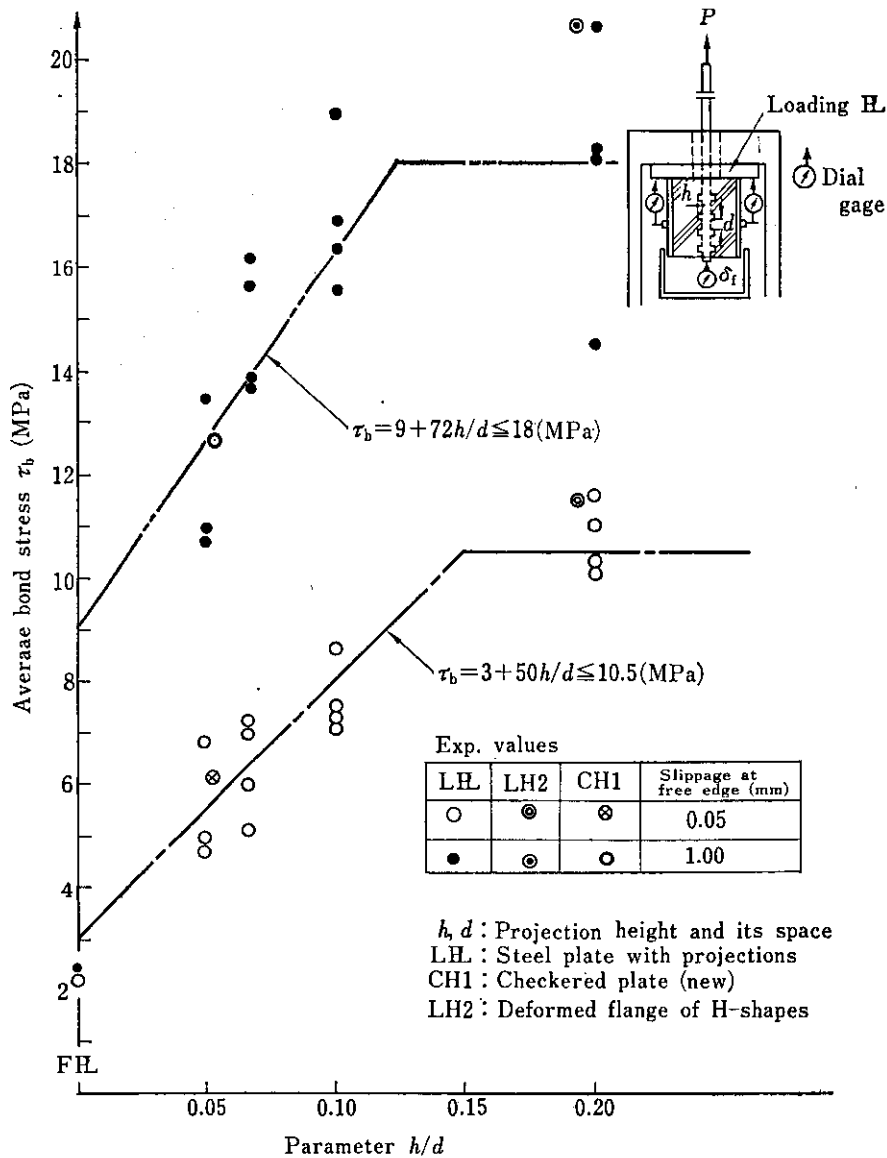


Fig. 5 Relation between average bond stress and parameter h/d

The relations of τ_b with h/d with respect to the checkered plate are also presented in Fig. 5. Since they are positioned in eq. (1), it is confirmed that eq. (1) is applicable to the bond strength of checkered plate with concrete. Therefore, high bond strength can be anticipated by enlarging h/d . However, in actual applications, there are limiting factors in manufacturing such as rolling load during rolling. Bond stress of commercial checkered plate corresponding to δ_f at 0.05 mm and 1.00 mm is respectively 2.8 and 5.3 times that of flat steel plate. It is confirmed that the commercial checkered plate can produce sufficient bond resistance with concrete.

3 Mechanical Property of Composite Checkered Steel Pipes

3.1 Bond Strength of Checkered Steel Pipe with Concrete⁴⁾

In order to check the extent of increase of the bond strength between checkered steel pipe and concrete over the bond strength between flat steel pipe and concrete, and further to examine the extent of influence of concrete strength and surface condition of checkered steel pipe on average bond stress, push-out tests on full-size test pieces were conducted as shown in Photo. 1.

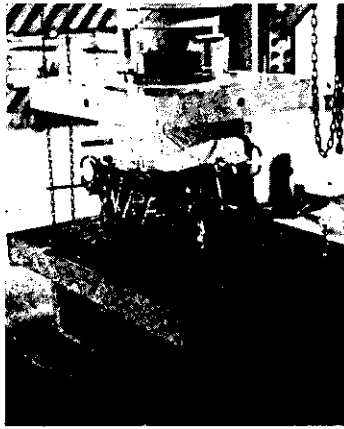


Photo. 1 Setup for push-out test of composite checkered steel pipe

3.1.1 Static push-out tests

Push-out tests were conducted on 9 types of test pieces including flat steel pipe for comparison so as to determine the relationship between push-out loads and slippage at free end. The standard test pieces were set to $\phi = 600 \text{ mm} \times t = 9 \text{ mm}$, bond length of $L = 300 \text{ mm}$ and design strength of concrete $\sigma_r = 30 \text{ MPa}$. Variations of this standard test piece include those with 200 and 600 mm for L , 15 and 45 MPa for σ_r , oil or mud coated surface of steel, and double steel pipe having checkered steel plate of $\phi_i = 500 \text{ mm} \times t_i = 9 \text{ mm}$ inside.

From Fig. 6 which shows bond stress (τ_b) corre-

sponding to $\delta_f = 0.05$ and 1.00 mm and maximum bond stress (τ_{bmax}), the following points have become clear.

- (1) The τ_{bmax} of the checkered steel pipe shows a 4.9 MPa, about 13 times τ_{bmax} of flat one.
- (2) When oil is coated on the surface of steel, its τ_{bmax} slightly decreases, whereas its τ_{bmax} lessens by about 20% when mud is coated.
- (3) Design strength of concrete exerts considerable influence on τ_{bmax} of the checkered steel pipe, and its ratio is roughly in proportion to its strength.

3.1.2 Push-out fatigue tests

From Fig. 7 which shows the relationships between the range of bond stress (τ_{br}), number of repeating cycles (N_c), and slippage (δ_f), the following point have become clear.

- (1) In the initial loading, a comparatively large residual slippage is generated. However, after the second loading, increases in residual and elastic slippage slow down. δ_f at the maximum load at 2 million cycles was about double δ_f at the initial maximum load.
- (2) When the minimum bond stress was set at 0.1 MPa, the maximum bond strength that could withstand 2 million cycles of repeated stress was 2.1 MPa. It is a high of 43% of the static maximum bond strength.
- (3) In view of safety in design, when the amount of slippage at the maximum load is set at 1.0 mm, allowable bond stress of 2.1 MPa can be adopted.

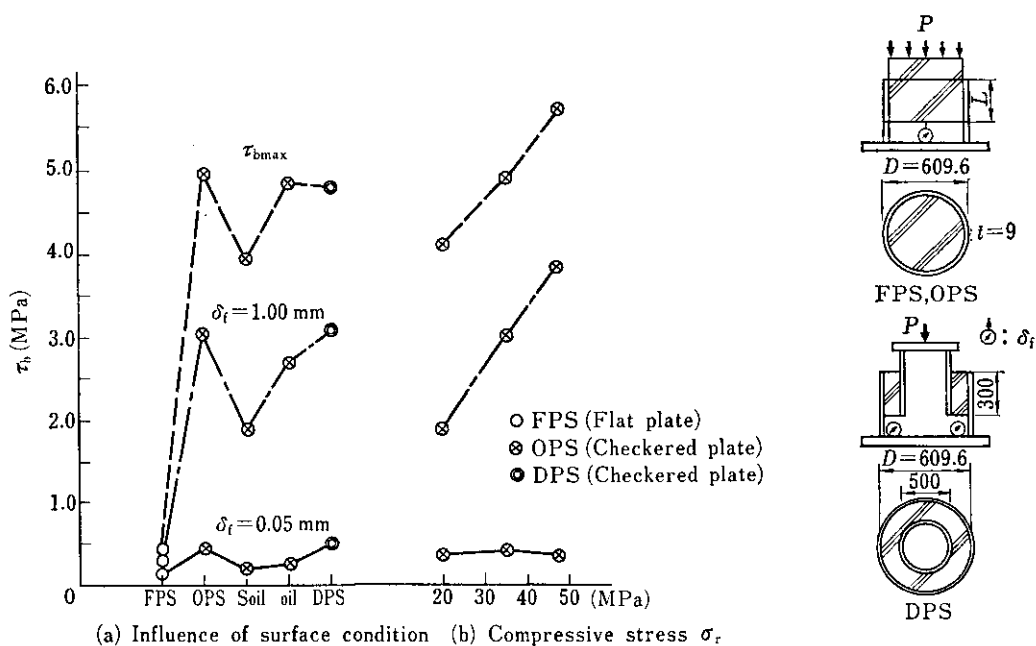


Fig. 6 Bond stress of composite steel pipes in pushout static tests

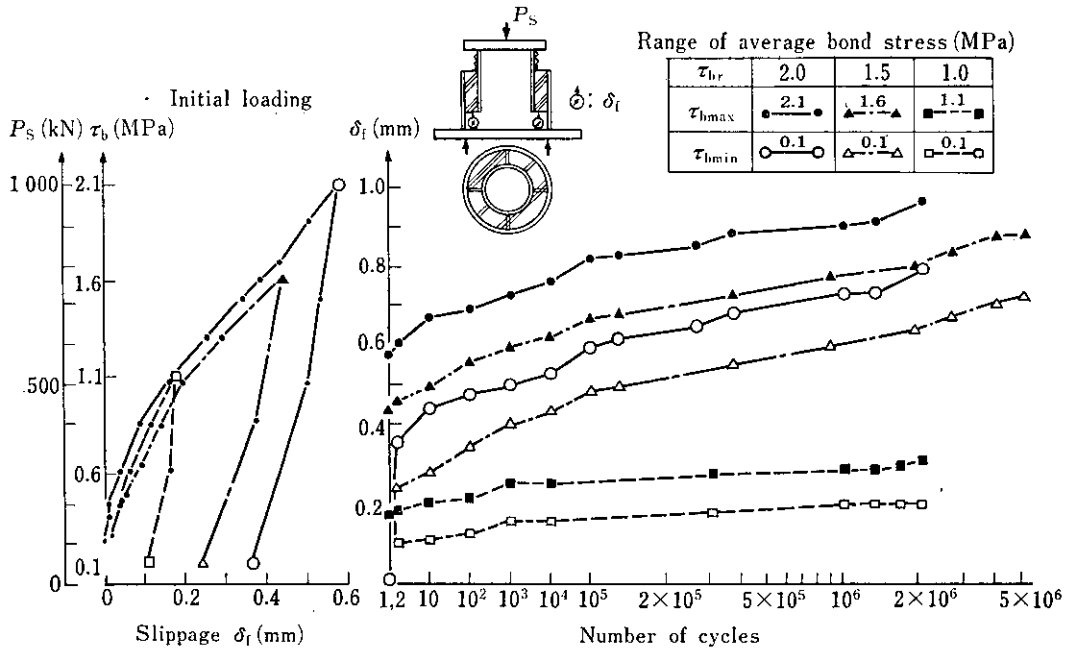


Fig. 7 Relation between N_f and δ_f for composite checkered steel pipes in push-out fatigue tests

3.2 Mechanical Property of Composite Piles

3.2.1 Outline of simple bending tests

Simple bending tests were conducted to obtain data on the bending strength and flexural rigidity when using checkered steel pipes as composite piles in the field.

Test pieces included two pieces each of checkered and flat steel pipe completely filled with concrete. The

maximum coarse aggregate size was also 25 mm in this test, and ready-mixed concrete with a design strength of 30 MPa was used.

As shown in Fig. 8, the composite pile beams were loaded at two points symmetrically positioned with respect to the center of the span. The load was gradually increased straight until significant local buckling was observed in the compressive region of the pipe or until the pipe's tensile strain reached 2%. At each

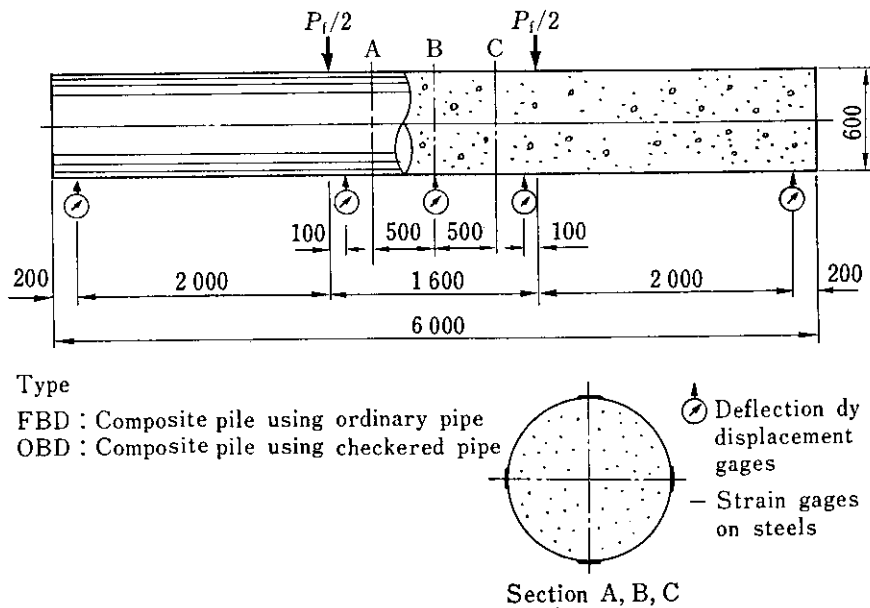


Fig. 8 Schema and types of composite pile specimens

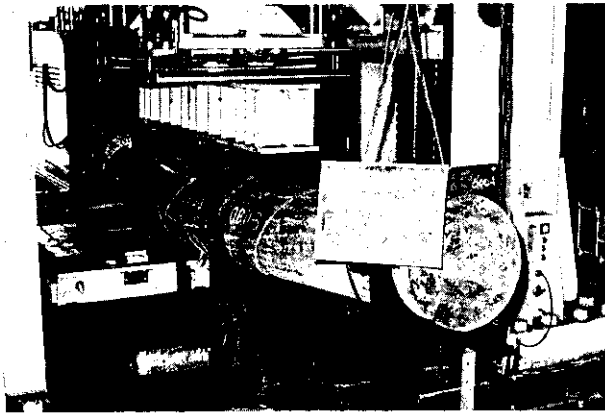


Photo. 2 Setup for bending test of composite pile

stage of load, extreme fiber stress, deflection at center of span, etc. were measured, and the load-strain and load-displacement curves were obtained for each test piece. Details of the load bearing tests are shown in Photo. 2.

3.2.2 Bending strength

M_{al} , M_{yi} , and M_{max} obtained from the extreme fiber stress of the pipe for each test piece are shown in Fig. 9. M_{al} and M_{yi} stand for the permissible bending moment when the pipe's extreme fiber stress reaches the allowable stress of steel of 140 MPa and the yield bending moment obtained from extreme fiber stress by using a 0.2% offset. M_{max} is the maximum resistance bending moment.

From these tests, the following points have been confirmed. The bending strength of the composite piles in the elastic region is about 1.2 times that of the steel pipe. However, as the tensile stress region of the

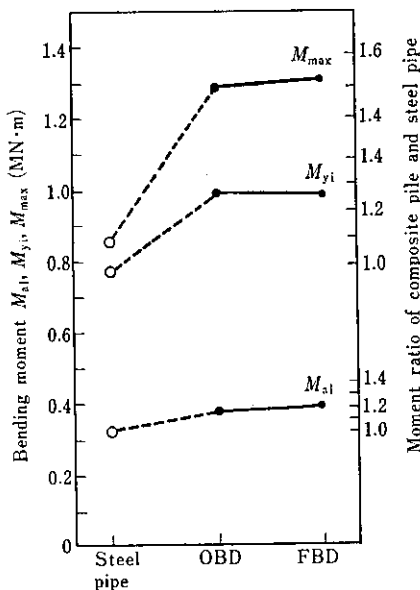


Fig. 9 Bending strength of composite piles

steel pipe begins to yield, the ratio of bending strength gradually rises to over 1.5 times that of the steel pipe in the final analysis, probably because of local buckling of the steel pipe being constrained by concrete.

3.2.3 Flexural rigidity

The relationship among bending moment M_p , flexural rigidity of the composite pile $E_s I_c$, and curvature ρ can be expressed as follows:

$$E_s I_c = \frac{M_p}{\rho} \dots \dots \dots (2)$$

Fig. 10 shows $E_s I_c$ corresponding to 500 kN·m of M_p obtained from the measured values of deflections of three points at load bearing points and at center of span. From this diagram, it is clear that the flexural rigidity of composite checkered pipe is about 10% higher than that of the composite pile using flat steel pipe and about 1.4 times the rigidity of steel pipe. On the other hand, when the elastic coefficient of concrete is set at 30 GPa while ignoring tensile stress of concrete, the flexural rigidity of the composite pile is calculated to be 200 MN·m². Since this result is in agreement with the flexural rigidity of the composite pile using flat steel pipe, the adequacy of this experiment is confirmed.

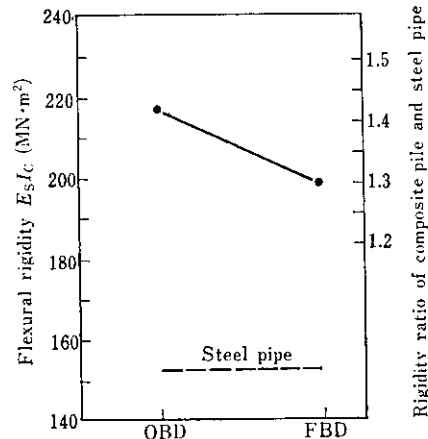


Fig. 10 Flexural rigidity of composite piles

4 Structural Characteristics of Encased Deformed Flange H Composite Beams

4.1 Merit of Deformed Flange H-shapes in Encased Composite Structures

The basic design concept in Japanese specifications of SRC structures adopts the method of accumulative allowable strength. However, since steel skeletons and reinforced concrete (called RC) members can be strained independently from each other, sectional

stress conditions can not be obtained, and also concrete encased steel skeletons (called SC) structures are outside the application range of this method.

In view of the fact that almost all main reinforcing bars in RC structures are deformed bars, the adoption of an RC calculation method in which flat H-shapes are assumed to have bonding strength equivalent to that of deformed bars involves an element of risk. Under these circumstances, deformed flange H-shapes with lateral projections are newly developed in order to secure reliable bonding and to positively incorporate the RC method in SRC and SC structures. With these types of H-shapes, not only are sectional stress conditions correctly known, but also workability improvement in concrete coverage in SC structures can be expected.

4.2 Mechanical Property on Static Flexure Tests

4.2.1 Maximum crack width of concrete

With attention being focused on the great influence steel-concrete bond characteristics have on maximum crack width (W_{cmax}) of concrete in beams, bending tests were made with SC and SRC specimens made of deformed flange H-shapes (see Photo. 3). Fig. 11 shows the schema and types of encased deformed flange and plan flange H composite beams for flexure tests.

The relationships between the calculated stresses as obtained by conventional calculation method (elastic

calculation in which the tensile stress of concrete is neglected, and its elasticity modulus is assumed to be 14 GPa) and W_{cmax} are shown in Fig. 12(a). Here, as for the value of W_{cmax} , the mean value of the two largest crack widths in the pure bend section was adopted.

The W_{cmax} of SC beams made of deformed flange H-shapes was approximately 25% smaller than that of SC beams made of flat flange H-shapes, and the allowable crack width corresponding to calculated stress on bottom flanges of 140 MPa was around 0.2 mm. Further, from the fact that the W_{cmax} of SC beams made of deformed flange H-shapes was nearly equivalent to that of RC beams made of deformed



Photo. 3 Setup for flexure test on SC beam with deformed flange H-shapes

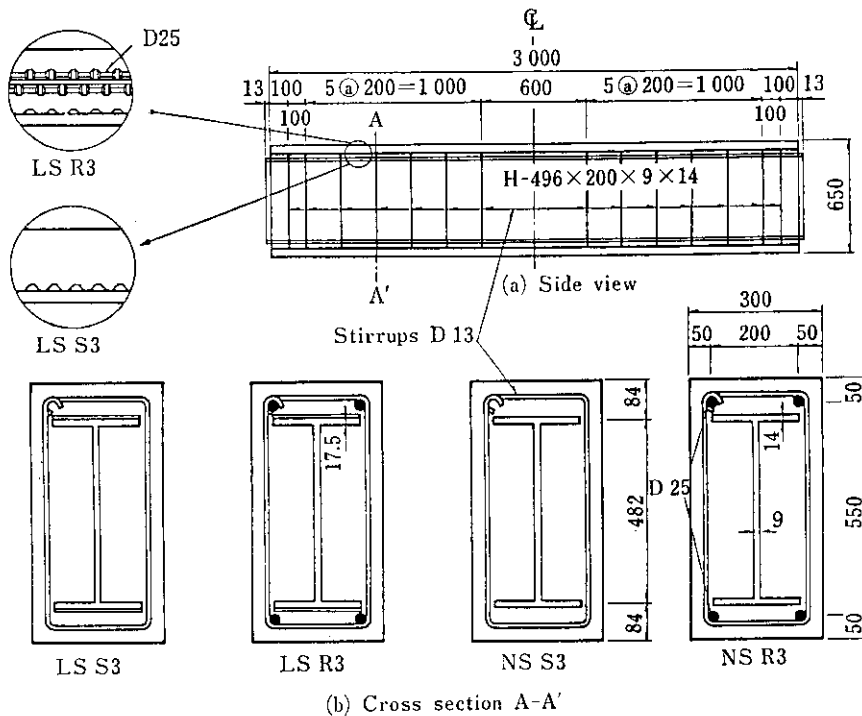
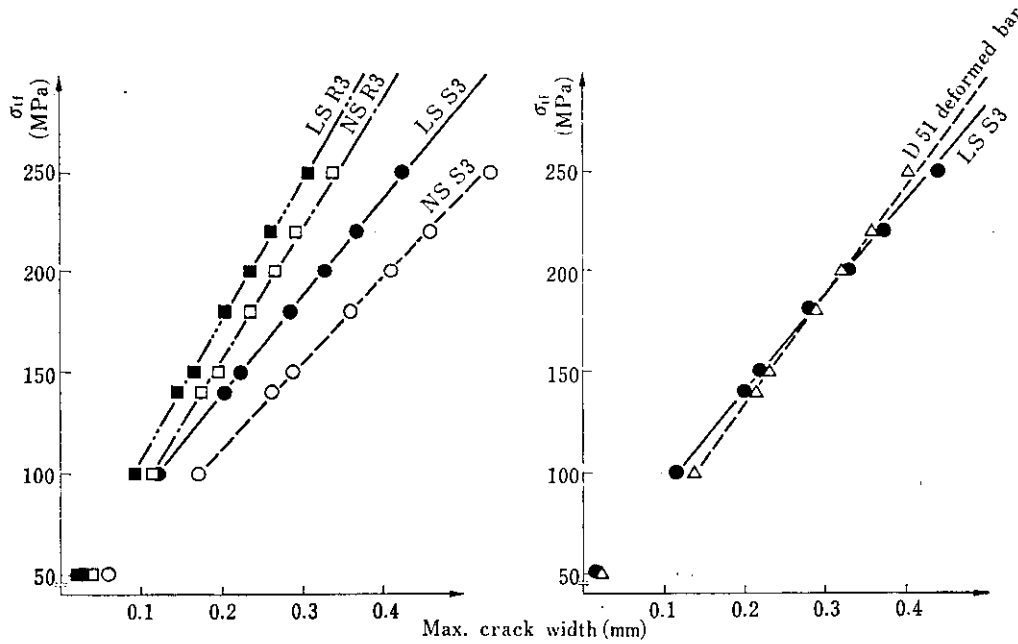


Fig. 11 Schema and types of SC and SRC specimens for flexure tests



(a) LS R3, NS R3, LS S3, NS S3 (b) Comparison of LS S3 with D51 deformed bar

Fig. 12 Relation between crack width and tensile fiber stress of H-shapes

bars, D51, as shown in Fig. 12(b), the mechanical equivalence of SC beams made of deformed flange H-shapes to RC structures made of D51 was confirmed, and also the possibility of adopting the same 180 MPa as the allowable tensile stress for SRC beams made of deformed flange H-shapes, as with D51, was confirmed.

4.2.2 Ultimate strength and slippage at beam end

As can be seen from Table 2, the ultimate strength of beams made of flat flange H-shapes is lower than that of beams made of deformed flange H-shapes, being 92% for SC beams and 93% for SRC beams. In Fig. 13, slippage between H-shapes and concrete

at beam end and the deflection at midspan of both types is compared, on the assumption that the difference is caused by the separation of concrete from H-shapes. With specimens NS S3 and NS R3 made of flat flange H-shapes, slippage was observed at the beam end at 80% ultimate strength load, and with the increase in slippage, the rigidity of these beams decreased in excess of that of specimens LS S3 and LS R3 made of deformed flange H-shapes. In contrast to this, with LS S3 and LS R3, the bond between deformed flange H-shapes and concrete was so good that even under ultimate stress conditions, no slippage was observed.

Table 2 Comparison of experimental values with calculated ones for ultimate loads

Specimen	Cal.values(kN)		Exp.values (kN)			$\frac{P_{slip}}{P_{fmax}}$	$\frac{P_{fmax}}{P_{uc1}}$	$\frac{P_{fmax}}{P_{uc2}}$
	Case 1*	Case 2*	Ultimate loads	Slipping loads	P_{fmax}			
	P_{uc1}	P_{uc2}	P_{fmax}	P_{slip}				
LS S3	1 213	1 441	1 543	—	—	1.27	1.07	
NS S3	1 213	1 441	1 425	1 137	0.80	1.17	0.99	
LS R3	1 594	1 874	1 921	—	—	1.20	1.02	
NS R3	1 594	1 874	1 784	1 450	0.81	1.12	0.95	

* Case 1 : $\sigma_{sy} = 245$ MPa, $\sigma_{ry} = 343$ MPa, $F_c = 0.85 \sigma_{ck}$
 * Case 2 : $\sigma_{sy} = 297$ MPa, $\sigma_{ry} = 391$ MPa, $F_c = 0.85 \sigma_{ck}$

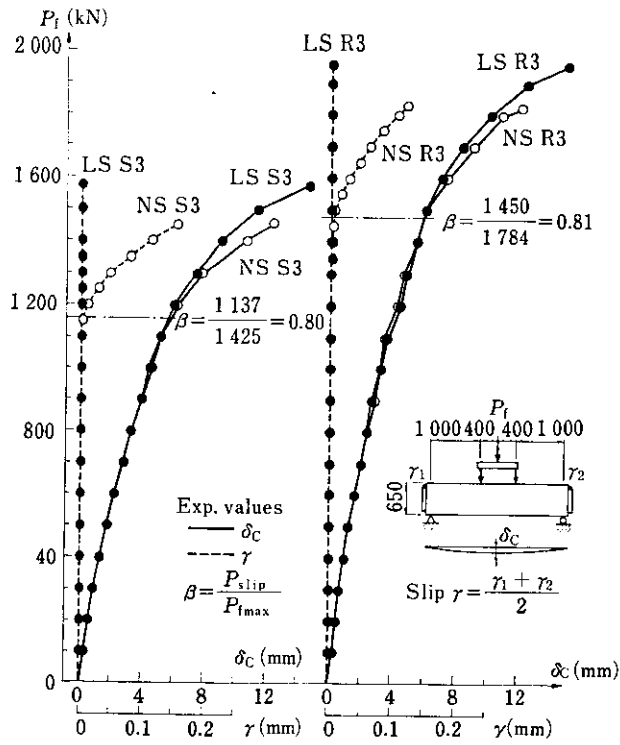


Fig. 13 P_f - δ_f and P_f - γ curves on SC, SRC beams

4.3 Fatigue Strength of Deformed Flange H-shapes in Beams

Bending fatigue test specimens for SC and SRC beams made of deformed flange H-shapes are shown in Fig. 14, and the S-N curves of the deformed flange H-shapes are shown in Fig. 15. Solid dots and double circles represent the empirical values of the beam shown in Fig. 14, and the broken line represents the empirical results of D51 in RC beams²¹.

As shown in Fig. 15, the 2×10^6 fatigue strength amplitude of deformed flange H-shapes in beams is estimated to be 184 MPa from the conventional calculation method, which is slightly lower than 192 MPa for D51 in RC beams, but still fully satisfies the permissible fatigue stress limit for deformed bars of 176 MPa.

5 Conclusion

The mechanical performances of composite checkered steel pipes and encased deformed flange H composite beams have been explained and can be summarized as follows:

- (1) The static maximum bond strength of checkered

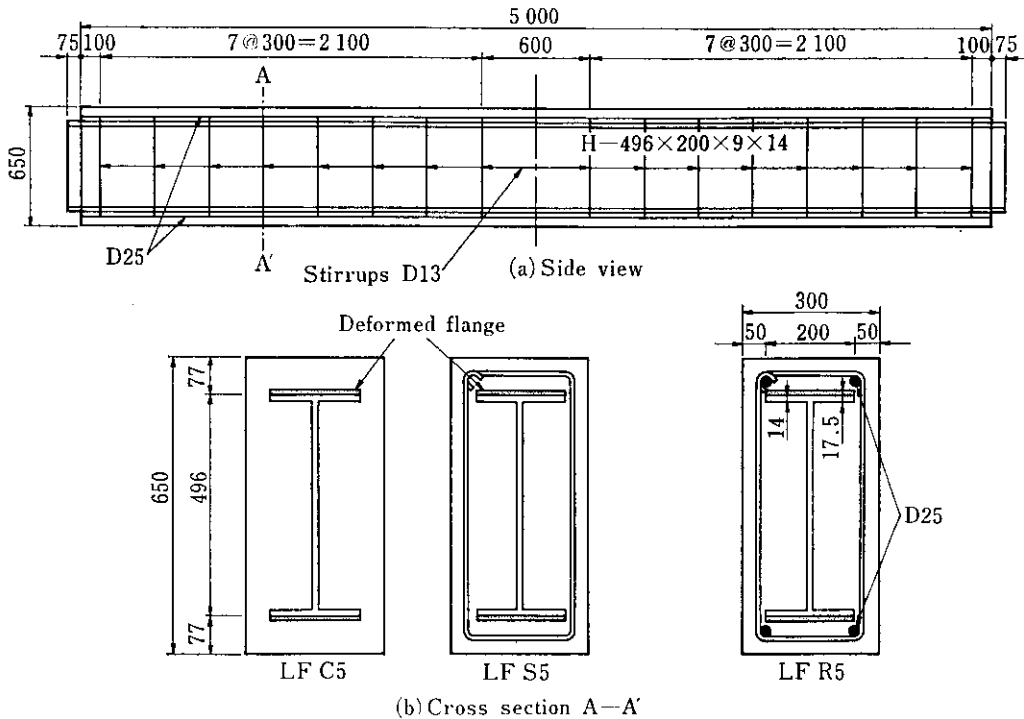


Fig. 14 Schema of SC and SRC with flange deformed H-shape for fatigue tests

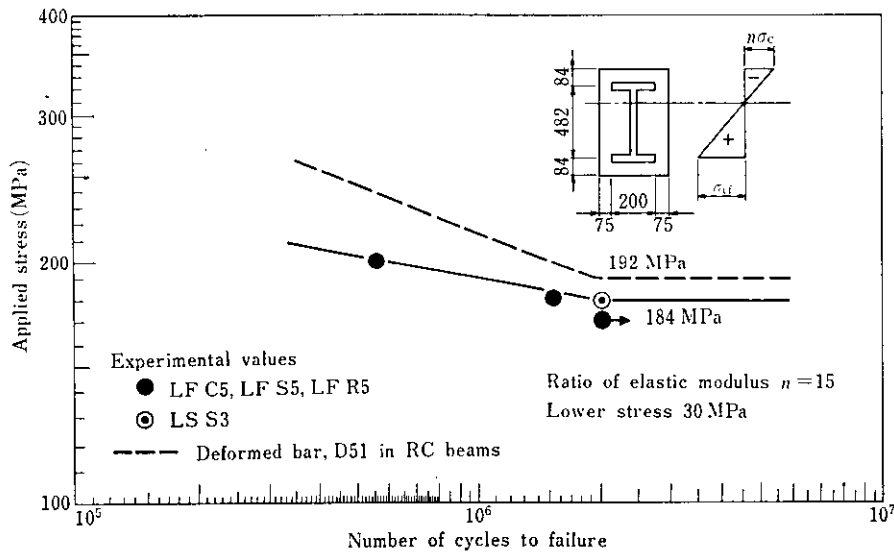


Fig. 15 S-N curves of deformed flange H-shapes in SC and SRC beams

- steel pipe with concrete was as high as 4.9 MPa, about 13 times that of flat steel pipe.
- (2) The range of bond strength that could withstand 2 million cycles of repeated load was 2.1 MPa. It is a high of 43% of the static maximum bond strength.
 - (3) By grouting concrete into checkered steel pipe, the unification of steel pipe with concrete is increased to such an extent that composite piles possessing a considerable sectional performance can be formed without using expansive admixtures.
 - (4) Maximum crack width of concrete on encased deformed flange composite beams is 25% smaller than that of SC beams with the flat flange H-shapes. This indicates that higher allowable stress can be adopted in design of encased beams by the use of deformed flange H-shapes.
 - (5) The bond between deformed flange H-shapes and concrete was so good that even under the ultimate strength for beams, no slippage was observed.

- (6) The mechanical property of the encased deformed flange H composite beams was found to be almost equivalent to that of RC beams using deformed bars, D51.

References

- 1) T. Okumura and M. Sato: "Analysis of Composite Beams Considering stiffness of Floor and Lateral Systems", *Trans. of JSCE*, Vol. 6 (1974), pp. 4-5
- 2) T. Yamasaki, M. Ishiwata and M. Sato: "Studies on Fatigue Characteristics of Large Diameter Deformed Bar D51 in Axial Loads and Reinforced Concrete Beams", *Trans. of JSCE*, Vol. 10 (1978), pp. 301-302
- 3) M. Sato and M. Ishiwata: "Bond Characteristics Between Concrete Flat or Lugged Steel Plate", *Trans. of JCI*, 2 (1980) IV-14, pp. 311-318
- 4) M. Sato, C. Kato and H. Miyoshi: "Mechanical Characteristics of Concrete-Filled Steel Pipes with Checkered Projections", *Trans. of JCI*, 3 (1981) VI-2, pp. 431-438